Journal of Alloys and Compounds 495 (2010) 149–153

Contents lists available at ScienceDirect

Journal of Alloys and Compounds

journal homepage: www.elsevier.com/locate/jallcom

Hydrogen storage in Mg–10 at.% $LaNi_5$ nanocomposites, synthesized by ball milling at different conditions

T. Spassov*, P. Delchev, P. Madjarov, M. Spassova, Ts. Himitliiska

1 James Bouchier Blvd., Faculty of Chemistry, University of Sofia, 1164 Sofia, Bulgaria

ARTICLE INFO

Article history:
Received 8 December 2009
Received in revised form 15 January 2010
Accepted 21 January 2010
Available online 1 February 2010

Keywords:
Mg-based composite
Hydrogen storage materials
Nanostructured materials
Ball milling
Gas-phase hydrogen sorption

ABSTRACT

Three Mg–10 at.% $LaNi_5$ nanocomposites were synthesized by high-energy ball milling at different conditions. One of the composites was prepared by milling MgH_2 and $LaNi_5$, whereas for the other two composites pure Mg and $LaNi_5$ were used as starting materials. The last two composites were milled at different conditions—dry milling and with heptane. Relatively narrow particle size distribution has been determined by scanning electron microscopy for all composites. Mean particle size of about 2 μm has been obtained for the first two composites, while the composite milled at milder mechanochemical conditions (in heptane) shows substantially larger average particle size of about 6 μm. All composites have shown nanocrystalline microstructure (28–33 nm), which appeared to be quite stable during hydriding/dehydriding cycling, slightly increasing the mean crystallite size regardless the high-temperature of annealing (300 °C). Formation of new phases has been detected during the milling and further annealing—Mg_2Ni and Mg_6Ni were formed. Hydriding and dehydriding kinetics were found to be very fast for the composites with finer particle and grain sizes. Partial low-temperature hydrogen absorption has been observed and "pump-getter" mechanism was suggested and proved.

1. Introduction

The usage of magnesium as a hydrogen storage material is limited by its relatively slow kinetics, high hydrogen absorption and desorption temperature and its susceptibility to oxidation. On the other hand $LaNi_5$ is a well-known material for both electrochemical and gas-phase applications, which easily absorbs and desorbs hydrogen even at room temperatures, but its limitations are low capacity, high specific weight and high price. One approach towards improving the H-sorption properties of Mg-based materials is reducing the particle size down to nanometer scale [1,2]. For coarse-grained polycrystalline MgH_2 it could take as long as several hours to decompose at 300–350 °C. Size reduction gives better results [3,4], but is often not sufficient and comes with the cost of sacrificing capacity for kinetics. Therefore research on catalyst additions [5–7], composites [8–12] and alloys [13,14] based on Mg (especially synthesized by reactive ball milling) has been intensively carried out. In our recent study [15] it was shown that in addition to the grain size, the particle reduction (to less than 1 μm) improves the hydrogen sorption kinetics of nanocrystalline Mg/MgH_2 powders.

$Mg–LaNi_x$ composites have been investigated widely both in terms of H-storage capacity [16–21] and thermodynamics of hydriding [22–24]. Certain common properties have been found, including the ability to achieve partial hydrogenation at room temperature and relatively high H-storage capacity (~4 wt.%).

Composites based on RE–Mg–Ni (RE: rare earth element) with $PuNi_3$ structure can absorb and desorb via gas-phase hydrogenation up to 1.8 wt.% hydrogen [25,26]. Electrochemical hydrogenation/dehydrogenation of those systems [27,28] proved that they appear to be a good potential candidates as negative electrode materials. In our previous study [29] it was found that nanocrystalline Mg–15 at.% $MmNi_5$, produced by planetary ball milling, shows maximum discharge capacity of 120 mAh/g (0.5 wt.% of hydrogen) under electrochemical hydrogenation. It was found that formation of $Mg(OH)_2$ impedes further hydrogen penetration and blocks the surface of the particles. Additional study carried out by isolation of the surface of $Mg–MmNi_5$ from the electrolyte shows capacity of 350 mAh/g, which is an evidence that during electrochemical charging both phases (Mg-rich and $MmNi_5$) are hydrogenated [30].

Studies on the $Mg–LaNi_5$ composites [25] show that the phase composition and microstructure influence critically on their hydrogen storage properties (kinetics, hydrogen capacity, low-temperature hydrogen absorption). Besides, decomposition of the $LaNi_5$–Mg composites during hydriding has been observed due to the increased diffusivity of the metal atoms in the presence of hydrogen [26]. Hence, the hydrogen storage properties of com-

* Corresponding author.
E-mail address: tspassov@chem.uni-sofia.bg (T. Spassov).

0925-8388/$ – see front matter © 2010 Elsevier B.V. All rights reserved.
doi:10.1016/j.jallcom.2010.01.107

Table 1
Composition and milling conditions for the composites studied.

Composite	Composition	Starting materials	Milling duration	Milling atmosphere	Milling conditions
C1	Mg–10 at.% $LaNi_5$	$MgH_2 + LaNi_5$	10 h	Ar	Dry milling
C2	Mg–10 at.% $LaNi_5$	$Mg + LaNi_5$	10 h	Ar	Dry milling
C3	Mg–10 at.% $LaNi_5$	$Mg + LaNi_5$	10 h	Ar	Milling in heptane

posites with different microstructure and particle and crystal size is important to be determined. Therefore the aim of the present study was the microstructural evolution of such composites during reactive mechanical milling at different milling conditions as well as during hydriding/dehydriding. Additionally, the low- and high-temperature hydriding and dehydriding of the Mg–10 at.% $LaNi_5$ nanocomposites were investigated.

2. Experimental

The composites were synthesized by ball milling, using a custom built planetary ball mill [11]. The milling process was carried out for 10 h with 1 h of continuous milling, followed by 30 min relaxation. One of the composites (denoted as C1) was prepared using pure MgH_2 (supplied by GKSS Research Center Geestacht GmbH) and commercial $LaNi_5$, whereas for the other two composites Mg (>99%) and $LaNi_5$ were used as starting materials. The last two composites were milled at different conditions—dry milling under Ar (composite C2) and milling in heptane under Ar (C3), Table 1. For this synthesis hardened Cr-steel vials were used as well as 6 mm steel balls, as the powder to ball (P/B) ratio was 1:8. The samples were investigated for contaminations with AAS, and the traces of Cr and Fe were found to be insignificant (Fe = 0.04 at.%, Cr = 0.006 at.%).

The handling and storage of the synthesized powders were performed in a glove box under Ar, however loading the specimen in the "pressure-composition-temperature" (PCT) apparatus for the gas-phase hydriding as well as the X-ray diffraction (XRD) experiments were realized in air, which may have resulted in a formation of a thin oxide layer (MgO) on the surface of the powders.

The hydrogen sorption behavior was investigated using Sievert's type (PCT) apparatus with samples from 100 to 150 mg. Structural information was obtained by XRD, using Cu-Kα radiation. Morphology and particle size distribution were obtained by scanning electron microscope (SEM) JEOL 5510 and using ImageJ software.

3. Results and discussion

The SEM micrographs (Fig. 1a) show for the composite C1 mean particle size of about 2 μm. Similar particle size distribution and average size are observed for the composite C2, whereas for the composite C3 the powder particles are larger (about 6 μm). Fig. 1b presents a typical SEM micrograph of the composite C3. Although a number of particles of greater size can be observed for all composites it is clearly seen at higher magnifications that these larger particles are actually agglomerates of much smaller ones (Fig. 1c). Moreover, extremely fine cold welded particles of less than 100 nm can also be detected for the composite C1 (Fig. 1d), which is not the case for the other two ball milled materials. Cracks can also be observed on the particles surface for all composites, which present good pathways for the hydrogen towards the particle inner parts.

The X-ray powder diffraction of the as-milled samples shows $LaNi_5$ phase only. No MgH_2 or Mg can be found on the diffractograms in Fig. 2. MgH_2 has decomposed during the milling process. The evidence for this was the increase of the pressure within the vials by 3 bar during the first 2–3 h of milling, most likely due to the released H_2, as a result of MgH_2 decomposition. The last was additionally proved by PCT desorption analysis of the as-milled composite C1. The diffraction peaks of Mg and Mg-based phases are very broad and strongly suppressed for all samples after 10 h of milling. Most probably the high-energy milling introduces large concentration of defects in the magnesium phases and strongly reduces their grain size. As it will be reported later in this study

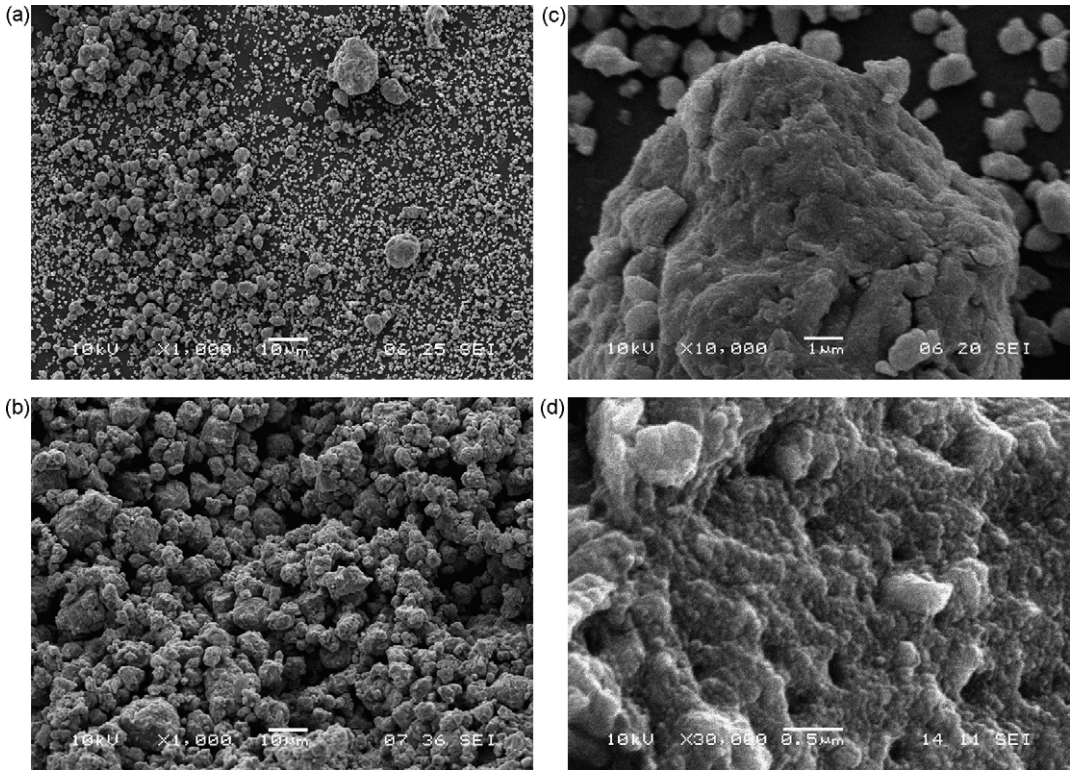

Fig. 1. SEM micrographs of the as-milled composites: C1 (a), C3 (b), C1 at higher magnifications (c) and (d).

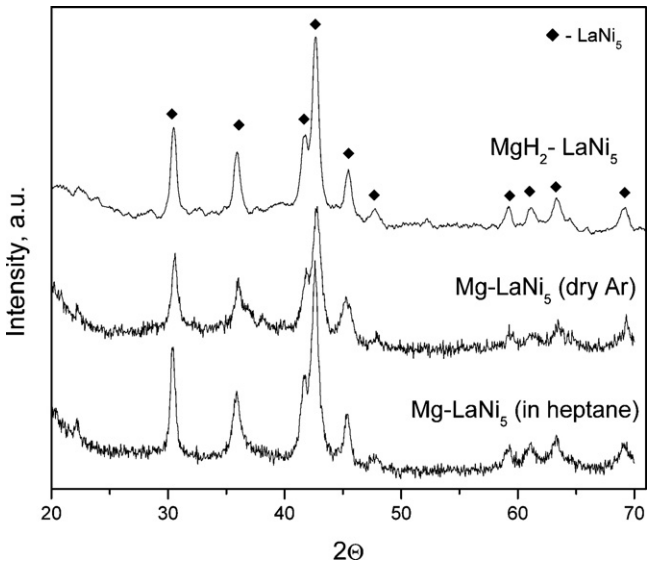

Fig. 2. X-ray diffractograms of the as-milled composites.

Mg_2Ni and Mg_6Ni phases were detected after annealing the ball milled composites. The mean crystallite size, calculated by the Scherrer equation is 28 ± 2 nm for the $LaNi_5$ phase (from the diffraction peaks at about 31 and 36° 2θ) in the composites C1 and C2 and 33 ± 2 nm for C3.

The composites' hydrogen sorption ability was studied in the Sievert's type apparatus. The temperature was kept at 300 °C (±3 °C) and the applied pressure was 8 bar (Figs. 3 and 4).

Fig. 3 reveals hydrogen absorption kinetic curves for the three composites at 300 °C. The absorption curves are obtained after activation of the materials, realized in this case by 3 preliminary hydrogen absorption/desorption cycles. The activation is mainly necessary due to the thin oxide layer on the surface of the particles, which has probably been formed during the samples handling. Formation of suitable adsorption sites on the surface of the particles is actually connected with a process of decripitation—enlarging the existing gaps and cracks on the particle surface, resulting in formation of fresh and active reaction surface. This assumption was later proved by X-ray powder diffraction measurements. Thus, highest hydrogen capacities of 4.0–4.3 wt.% as well as fastest kinetics for all composites were measured after 2–3 hydrogen absorption/desorption cycles. The composites C1 and C2 reveal slightly higher capacity (4.3 wt.%) than the composite C3, which shows capacity of 4.1 wt.%. At later cycles (more than 10) the hydriding kinetics gets a little faster, but capacity is slowly decayed. The reason is decripitation again—creating new reaction surfaces by the crystal lattice fracturing results in hydrogen sorption acceleration, but at the same time it reduces the quantity of the interstitial sites suitable for hydrogen atoms accommodation. Generally, the absorption kinetics are very fast for all nanocomposites studied, reaching 50% of hydriding within the first 100–200 s. Preliminary estimations suggest diffusion-controlled mechanism of the H-absorption process. The higher hydrogen absorption rate for the composites C1 and C2 can be attributed to their noticeably smaller particle and grain sizes compared to those of the composite C3, milled at milder conditions (in heptane).

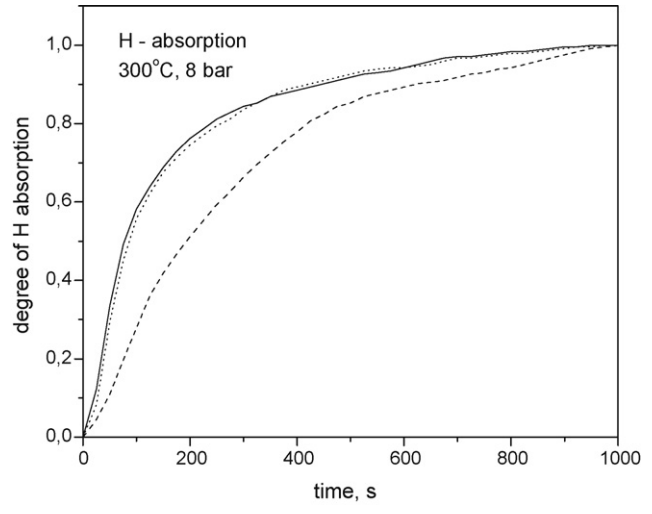

Fig. 3. PCT hydrogen absorption curves of the Mg-$LaNi_5$ nanocomposites (C1—solid line; C2—dot; C3—dash).

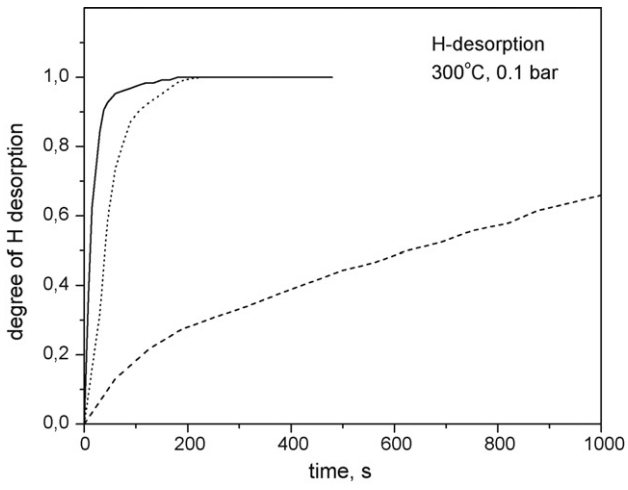

Fig. 4. PCT hydrogen desorption curves of the Mg–$LaNi_5$ nanocomposites (C1—solid line; C2—dot; C3—dash).

The desorption of hydrogen shows markedly different behavior of the composites C1 and C2 compared to C3 (Fig. 4). The kinetics are extremely fast after the first cycle of activation for C1 and C2—50% of the process takes place reproducibly during the first 40–50 s, whereas for C3 about an hour is needed for complete hydriding. One of the reasons for such behavior includes the finer grain and particle sizes in the first two composites. Additionally, as it will be later shown by XRD of the annealed samples the composites C1 and C2 contain larger amount of Mg_2Ni phase compared to composite C3, in which the metastable Mg_6Ni phase was detected. The observed differences in the phase composition of the materials milled under different conditions have certainly an effect on their hydriding/dehydriding kinetics as well.

An effect of low-temperature hydrogen absorption was also observed for the nanocomposites studied. If left for a few hours at temperature of about 40–45 °C under 8 bar of pure hydrogen pressure, the composite partially absorbs hydrogen. Such low-temperature hydrogen charging does not lead to high storage capacity, however it is still about 3–3.5 wt.%, but requires much longer time than absorption at 300 °C. X-ray diffraction data show presence of different phases in the composites after hydrogen absorption/desorption (Fig. 5). For the composite prepared from MgH_2 and $LaNi_5$, after hydrogen desorption at 300 °C, there are just two intermetallic phases that can be indexed undoubtedly—Mg_2Ni and $LaNi_5$, which actually means that the initial $LaNi_5$ has partially disproportioned, donating some of its Ni for the formation of Mg_2Ni. The nearest to $LaNi_5$ La–Ni phase is $LaNi_3$, which unfortunately, cannot be clearly identified since all of its most intensive peaks would be overlapped. The presence of Mg_2NiH_4 in the samples after high-temperature and low-temperature hydrogen absorption

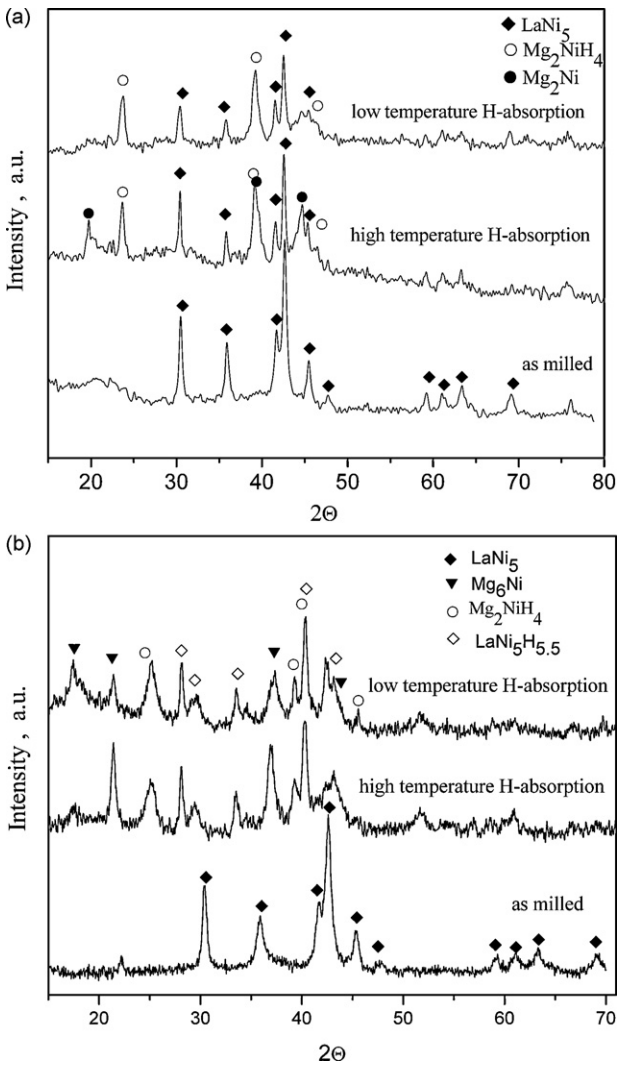

Fig. 5. XRD patterns of the samples in as-milled state and after different treatment (low-temperature hydriding at 40 °C and high-temperature hydriding at 300 °C): C1 (a) and C3 (b).

was clearly observed (Fig. 5a). It is also shown that formation of well-crystallized Mg_2Ni phase was only possible after appropriate annealing; annealing at about 50 °C of the ball milled samples does not result in clear Mg_2Ni formation. The composite prepared by milling Mg and $LaNi_5$ in heptane (C3) reveals somehow different phase evolution during milling and subsequent hydriding/dehydriding at 300 °C, Fig. 5b. Formation of Mg_2NiH_4 and metastable Mg_6Ni phase was detected, revealing that the last phase practically does not form hydrides at these conditions, a fact, which was also confirmed by Teresiak et al. [31]. This can also contribute to the deteriorated hydrogen sorption properties of the composite prepared in heptane. The presence of $LaNi_5H_{5.5}$ phase in the composite C3 after hydriding, Fig. 5b, is due to the cooling to room temperature under 8 bar of hydrogen in the PCT device.

To explain the effect of low-temperature H-absorption in the nanocomposites studied a pump-getter mechanism of the hydriding process was suggested. Since $LaNi_5$ easily absorbs hydrogen at room temperatures and releases it at temperatures as low as 30 °C, there is a good chance that the hydrogen is absorbed by $LaNi_5$ and then released. When released the hydrogen is in atomic form. However, since the Mg-based phases are in intimate contact with $LaNi_5$, certain quantities of pure, very active atomic hydrogen can be absorbed by them at room temperature. To check this hypothesis another experiment was done. The composite was sealed under argon at room temperature and consequently exposed to dynamic vacuum to purify it from the absorbed during the loading gases and water. After that the atmosphere was changed to 5 bar of pure H_2. After exposing the composite to that atmosphere for 15 min the system was heated to 100 °C (at such conditions none of the Mg-based phases would absorb H_2) for 5 min, which is enough for the $LaNi_5$ to release the absorbed H_2 and then cooled again to room temperature quickly by using water. This procedure was repeated three times and the sample was again purged with pure argon. The XRD pattern of the so-treated composite is similar to that of the low-temperature (40 °C) hydridied sample (Fig. 5a). Thus we can conclude that the pump-getter mechanism actually takes place in the hydriding process of the investigated nanocomposites.

4. Conclusions

Mg–10 at.% $LaNi_5$ composites were synthesized by high-energy ball milling at different conditions and using different initial substances (see Table 1). All composites show a relatively narrow particle size distribution with mean particle size of about 2 μm for C1 and C2 and about 6 μm for C3. The composites have shown nanocrystalline microstructure, which appeared to be quite stable during hydriding/dehydriding at 300 °C—slight increase of the mean crystallite size with few nm was only observed. Formation of new phases (Mg_2Ni and Mg_6Ni) has been detected during milling and subsequent annealing of the composites.

Hydriding and dehydriding kinetics were found to be very fast for C1 and C2, reaching 0.035–0.04 wt.%/s, as the explanation is the fine particle and grain size, appropriate phase composition and microstructure. A low-temperature hydrogen absorption has been observed for the composite C1 and pump-getter mechanism was suggested and proved. It was found that $LaNi_5$ does not decompose completely during milling and subsequent hydriding/dehydriding and has a positive effect on the low-temperature hydrogenation of the composites.

Acknowledgements

The work has been supported by the Bulgarian Scientific Research Fund under grant DO 02-226/2008 and by Bulgarian Scientific Research Fund under grant DO 02-82/2008, Project “Union”.

References

[1] G. Liang, J. Huot, S. Boily, A. Van Neste, R. Schulz, J. Alloys Compd. 291 (1999) 295–299.
[2] X.-L. Wang, S. Suda, Int. J. Hydrogen Energy 17 (1992) 139–147.
[3] J. Huot, G. Liang, S. Boily, A. Van Neste, R. Schulz, J. Alloys Compd. 293–295 (1999) 495–500.
[4] K.J. Gross, D. Chartouni, E. Leroy, A. Zuttel, L. Schlapbach, J. Alloys Compd. 269 (1998) 259–270.
[5] W. Oelerich, T. Klassen, R. Bormann, J. Alloys Compd. 315 (2001) 237–242.
[6] G. Liang, J. Huot, S. Boily, R. Schulz, J. Alloys Compd. 305 (2000) 239–245.
[7] G. Barkhordarian, T. Klassen, R. Bormann, J. Alloys Compd. 364 (2004) 242–246.
[8] J. Bobet, B. Chevalier, B. Darriet, J. Alloys Compd. 330–332 (2002) 738–742.
[9] Q. Liu, L.F. Jiao, H.-T. Yuan, Y.-J. Wang, Y. Feng, J. Alloys Compd. 427 (2007) 275–280.
[10] E. Grigorova, M. Khristov, M. Khrussanova, P. Peshev, J. Alloys Compd. 414 (2006) 298–301.
[11] P. Delchev, T. Himitliiska, T. Spassov, J. Alloys Compd. 417 (2006) 85–91.
[12] M. Au, Mater. Sci. Eng. B 117 (2005) 37–44.
[13] P. Delchev, P. Solsona, B. Drenchev, N. Drenchev, T. Spassov, M.D. Baró, J. Alloys Compd. 388 (2005) 98–103.
[14] A. Gasiorowski, W. Iwasieczko, D. Skoryna, H. Drulis, M. Jurczyk, J. Alloys Compd. 364 (2004) 283–288.
[15] D. Fátay, Á. Révész, T. Spassov, J. Alloys Compd. 399 (2005) 237–241.
[16] G. Liang, J. Huot, S. Boily, A. Van Neste, R. Schulz, J. Alloys Compd. 268 (1998) 302–307.
[17] T. Kohno, H. Yoshida, F. Kawashima, T. Inaba, I. Sakai, M. Yamamoto, M. Kanda, J. Alloys Compd. 311 (2000) L5–L7.

[18] T. Yamamoto, H. Inui, M. Yamaguchi, K. Sato, S. Fujitani, I. Yonezu, K. Nishio, Acta Mater. 45 (1997) 5213–5221.
[19] M. Terzieva, M. Khrussanova, P. Peshev, J. Alloys Compd. 267 (1998) 235–239.
[20] M. Zhu, C.H. Peng, L.Z. Ouyang, Y.Q. Tong, J. Alloys Compd. 426 (2006) 316–321.
[21] H. Reule, M. Hirscher, A. Weißhardt, H. Kronmuller, J. Alloys Compd. 305 (2000) 246–252.
[22] T. Kodama, J. Alloys Compd. 289 (1999) 207–212.
[23] T. Ivanova, R. Sirotina, V. Verbetsky, J. Alloys Compd. 253–254 (1997) 210–211.
[24] C. Colinet, J. Alloys Compd. 225 (1995) 409–422.
[25] K. Kadir, T. Sakai, I. Uehara, J. Alloys Compd. 302 (2000) 112–117.
[26] J. Chen, H.T. Takeshita, H. Tanaka, N. Kuriyama, T. Sakai, I. Uehara, M. Haruta, J. Alloys Compd. 302 (2000) 304–313.
[27] J. Chen, N. Kuriyama, H.T. Takeshita, H. Tanaka, T. Sakai, M. Haruta, Electrochem. Solid-State Lett. 3 (6) (2000) 249–252.
[28] B. Liao, Y.Q. Lei, G.L. Lu, L.X. Chen, H.G. Pan, Q.D. Wang, J. Alloys Compd. 356–357 (2003) 746–749.
[29] A. Borissova, S. Bliznakov, T. Spassov, J. Alloys Compd. 434–435 (2007) 760–763.
[30] S. Bliznakov, N. Dimitrov, T. Spassov, A. Popov, Mater. Res. Soc. Symp. Proc. 1042 (2008) 59–63.
[31] A. Teresiak, M. Uhlemann, J. Thomas, A. Gebert, Alloys Compd. 475 (1–2) (2009) 191–197.